IJAME
Int. J. of Applied Mechanics and Engineering, 2025, vol.30, No.3, pp.128-141
DOI: 10.59441/ijame/207141

STUDY ON THE INFLUENCE OF SLIDING BEARING STIFFNESS ON THE DYNAMIC RESPONSE OF HYDRO-GENERATOR SHAFT

Y. Ri*, S. Ryang, and G. Ryong
Umjong, Institute of Mechanic, KOREA (NORTH)
E-mail: ryj1989@star-co.net.kp

The dynamic modeling of the main shaft system of a hydro turbine generator is carried out by considering the combined effects of unbalanced mass force, magnetic pull force, hydrodynamic force and oil film force of the sliding bearing, its critical rotational speed is obtained, the effect of the sliding bearing stiffness at each journal on the critical rotational speed of the whole shaft system is evaluated, and the method is proposed to improve the stability of the hydro turbine generator by changing it, and the validity is demonstrated by the field test results.

Key words: hydro-turbine generator, dynamic modeling, critical rotational speed, sliding bearing stiffness.

1. Introduction

The determination of the critical rotational speed of a hydro-turbine generator under the combined action of mechanical, magnetic and hydraulic forces and the correct evaluation of the influence of these factors are important issues in hydro-turbine generator stability studies.

In [1-2], the nonlinear coupled vibration characteristics of a four-DOF system are investigated by numerical methods under the influence of mechanical forces, such as bearing looseness, misalignment, static unbalance, and oil-bearing blockage, in a vertical rotor-shaft-support system that models the rotor system of a hydro-turbine generator. In [3-9], the influence of various factors on the vibration response of the system in a four-DOF hydro turbine generator shaft system is analyzed by considering the unbalanced magnetic pull force and the unbalance force in the hydro-dynamic system composed of the generator rotor, hydro-turbine, shaft and support bearings.

Also some analyses were carried out on the natural vibration characteristics of the main system of the hydro-turbine generator unit with complex rotor bearing system and proposed a lot of methods to calculate the critical speed of the dynamic shaft system [10-14].

But there are still no papers that studied effect of sliding bearing stiffness on the critical rotational speed of the hydro turbine generator shaft system.

Therefore in this paper we investigate the dynamic modeling of the hydraulic turbine generator spindle system and the method of finding the critical rotational speed by considering the combined action of mass unbalance force, magnetic pull force, hydrodynamic force and oil film force of the sliding bearing, and shows the method to achieve the vibration stability of the system by evaluating the effect of sliding bearing stiffness on the critical rotational speed of the system.

2. Dynamic modeling of the hydro-turbine generator spindle system

The hydro-turbine generator spindle system considered in this paper consists of a generator rotor, a turbine, and three sliding bearings supporting the shaft and the shaft connecting them (Fig.1).
Take the coordinate system as shown in Fig.1 and neglect the torsional or axial vibration of the hydro-turbine generator shaft system and consider only the bending vibration.

* To whom correspondence should be addressed

$o_i(i=1,2,3,4,5)$ denote the center of the upper bearing 1, generator rotor 2, lower bearing 3, turbine bearing 4, and turbine 5, respectively, and $f_{x1}, f_{y1}, f_{x3}, f_{y3}, f_{x4}, f_{y4}$ are the oil film components of the bearings, p_{x2}, p_{y2} is the component of the magnetic tensile force, p_{x5}, p_{y5} is the component of the hydrodynamic excitation force, m_1, m_3, m_4 is the mass of each slide bearing, m_2, m_5 is the mass of the rotor and the turbine.

The free vibration equation of the system is expressed as [1, 2]:

$$[M_r]\{\ddot{X}_r\}+[\omega_r G_r + C_r]\{\dot{X}_r\}+[K_r]\{X_r\}=0\,. \tag{2.1}$$

In Eq.(2.1), X_r is the degree of freedom vector, is the velocity vector, and is the velocity vector.

$$\{X_r\}=[X^T\ Y^T]^T,\ \{X\}=[x_1\ \theta_{y1}\ x_2\ \theta_{y2}\ x_3\ \theta_{y3}\ x_4\ \theta_{y4}\ x_5\ \theta_{y5}]^T,$$

$$\{Y\}=[y_1\ -\theta_{x1}\ y_2\ -\theta_{x2}\ y_3\ -\theta_{x3}\ y_4\ -\theta_{x4}\ y_5\ -\theta_{x5}]^T.$$

The rotational angles around the x and y axes of the system are:

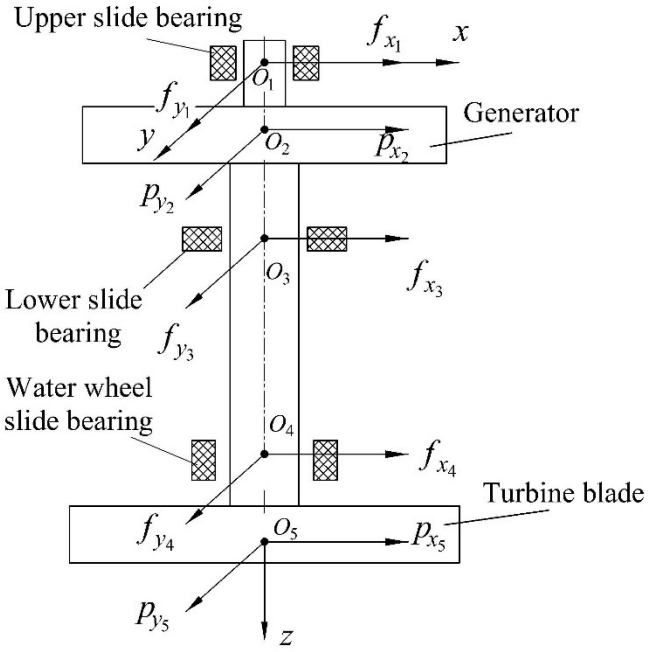

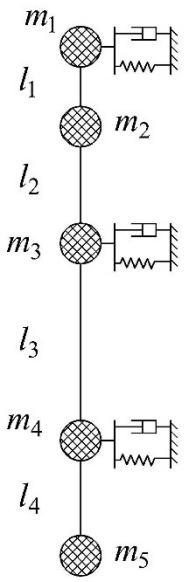

a) Fundamental structure. b) Dynamic model.

Fig.1. Mechanical model of the hydro-turbine generator shaft system.

M_r is the mass matrix of the system, ω_r is the angular velocity of the shaft system, G_r is the gyroscopic matrix, C_r is the damping matrix, K_r is the stiffness matrix, and the detailed form is as follows:

$$M_r=\begin{bmatrix} M_x & 0 \\ 0 & M_y \end{bmatrix},\quad G_r=\begin{bmatrix} 0 & G_x \\ G_y & 0 \end{bmatrix},\quad C_r=\begin{bmatrix} C_x & 0 \\ 0 & C_y \end{bmatrix},\quad K_r=\begin{bmatrix} K_x & 0 \\ 0 & K_y \end{bmatrix},$$

$$M_x = M_y, \quad K_x = K_y, \quad G_x = -G_y, \quad C_x = C_y, \quad M_x = diag[m_i \;\; J_{di}],$$

$$G_x = diag[0 \;\; J_{pi}], \quad C_x = diag[c_{ei} \;\; c_{di}], \quad i = 1,2,3,4,5$$

where, J_{di}, J_{pi} are the axial and polar moments of inertia of mass i, respectively, and K_x is the following matrices:

$$K_{x_{11}} = \begin{bmatrix} \frac{12EI_1}{l_1^3} & \frac{6EI_1}{l_1^2} & -\frac{12EI_1}{l_1^3} & \frac{6EI_1}{l_1^2} & 0 \\ \frac{6EI_1}{l_1^2} & \frac{4EI_1}{l_1} & -\frac{6EI_1}{l_1^2} & \frac{2EI_1}{l_1} & 0 \\ -\frac{12EI_1}{l_1^3} & -\frac{6EI_1}{l_1^2} & \frac{12EI_1}{l_1^3}+\frac{12EI_2}{l_2^3} & -\frac{6EI_1}{l_1^2}+\frac{6EI_2}{l_2^2} & -\frac{12EI_2}{l_2^3} \\ \frac{6EI_1}{l_1^2} & \frac{2EI_1}{l_1} & -\frac{6EI_1}{l_1^2}+\frac{6EI_2}{l_2^2} & \frac{4EI_1}{l_1}+\frac{4EI_2}{l_2} & -\frac{6EI_2}{l_2^2} \\ 0 & 0 & -\frac{12EI_2}{l_2^3} & -\frac{6EI_2}{l_2^2} & \frac{12EI_2}{l_2^3}+\frac{12EI_3}{l_3^3} \end{bmatrix},$$

$$K_{x_{21}} = \begin{bmatrix} 0 & 0 & -\frac{12EI_2}{l_2^3} & -\frac{6EI_2}{l_2^2} & \frac{12EI_2}{l_2^3}+\frac{12EI_3}{l_3^3} \\ 0 & 0 & \frac{6EI_2}{l_2^2} & \frac{2EI_2}{l_2} & -\frac{6EI_2}{l_2^2}+\frac{6EI_3}{l_3^2} \\ 0 & 0 & 0 & 0 & -\frac{12EI_3}{l_3^3} \\ 0 & 0 & 0 & 0 & \frac{6EI_3}{l_3^2} \\ 0 & 0 & 0 & 0 & 0 \end{bmatrix},$$

$$K_{x_{12}} = \begin{bmatrix} 0 & 0 & 0 & 0 & 0 \\ 0 & 0 & 0 & 0 & 0 \\ \frac{6EI_2}{l_2^2} & 0 & 0 & 0 & 0 \\ \frac{2EI_2}{l_2} & 0 & 0 & 0 & 0 \\ -\frac{6EI_2}{l_2^2}+\frac{6EI_3}{l_3^2} & -\frac{12EI_3}{l_3^3} & -\frac{12EI_3}{l_3^3} & 0 & 0 \end{bmatrix},$$

$$K_{x_{22}}=\begin{bmatrix} \frac{4EI_2}{l_2}+\frac{4EI_3}{l_3} & -\frac{6EI_3}{l_3^2} & \frac{2EI_3}{l_3} & 0 & 0 \\ -\frac{6EI_3}{l_3^2} & \frac{12EI_3}{l_3^3}+\frac{12EI_4}{l_4^3} & -\frac{6EI_3}{l_3^2}+\frac{6EI_4}{l_4^2} & -\frac{12EI_4}{l_4^3} & \frac{6EI_4}{l_4^2} \\ \frac{2EI_3}{l_3} & -\frac{6EI_3}{l_3^2}+\frac{6EI_4}{l_4^2} & \frac{4EI_3}{l_3}+\frac{4EI_4}{l_4} & -\frac{6EI_4}{l_4^2} & \frac{2EI_4}{l_4} \\ 0 & -\frac{12EI_4}{l_4^3} & -\frac{6EI_4}{l_4^2} & \frac{12EI_4}{l_4^3} & -\frac{6EI_4}{l_4^2} \\ 0 & \frac{6EI_4}{l_4^2} & \frac{2EI_4}{l_4} & -\frac{6EI_4}{l_4^2} & \frac{4EI_4}{l_4} \end{bmatrix},$$

$$K_x=\begin{bmatrix} K_{x_{11}} & K_{x_{12}} \\ K_{x_{21}} & K_{x_{22}} \end{bmatrix}. \tag{2.2}$$

Where E is the Young's modulus of the shaft material, I_i is the axial moment of inertia of the cross section of shaft i, and l_i is the length of shaft link E_i. Under assumption of elastic support, the sliding bearing support condition can be expressed through the generalized force.

$$\begin{Bmatrix} Q_{1d}^h \\ Q_{2d}^h \end{Bmatrix}=-\begin{bmatrix} c_{xx} & c_{xy} \\ c_{yx} & c_{yy} \end{bmatrix}\begin{Bmatrix} \dot{x}_j \\ \dot{y}_j \end{Bmatrix}-\begin{bmatrix} k_{xx} & k_{xy} \\ k_{yx} & k_{yy} \end{bmatrix}\begin{Bmatrix} x_j \\ y_j \end{Bmatrix} \tag{2.3}$$

Transferring this generalized force to the left-hand side of Eq.(2.1) and synthesizing it into the corresponding elements of the stiffness matrix and damping matrix, it is superimposed on the rows and columns corresponding to the bearing positions in the original stiffness matrix or damping matrix.
The unbalanced magnetic pull force caused by various causes, such as non-concentric rotor-stator coupling, rotor or stator pole imperfections, and shaft initial bending, is expressed by the following equation, considering that the pole pair number *p* of the hydro-turbine generator is generally greater than *3* [3-5].

$$\begin{bmatrix} F_{x\_ump} \\ F_{y\_ump} \end{bmatrix}=\frac{R_r L_r \pi k_j^2 I_j^2}{4\mu_0}\left(2\Lambda_0\Lambda_1+\Lambda_1\Lambda_2+\Lambda_2\Lambda_3\right)\begin{bmatrix} \cos\gamma \\ \sin\gamma \end{bmatrix}. \tag{2.4}$$

Where, μ_0 is the magnetic induction coefficient in the air, I_j is the field current of the generator rotor, K_j is the air gap fundamental magnetic intensity coefficient, R_r is the radius of the generator rotor, L_r is the length of the rotor, and the expansion coefficient Λ_n is:

$$\Lambda_n=\begin{cases} \frac{\mu_0}{\delta_0}\frac{1}{\sqrt{1-\varepsilon_2^2}} & (n=0), \\ \frac{\mu_0}{\delta_0}\frac{1}{\sqrt{1-\varepsilon_2^2}}\left[\frac{1-\sqrt{1-\varepsilon_2^2}}{\varepsilon_2}\right]^n & (n>0). \end{cases} \tag{2.5}$$

δ_0 is the average air-gap of the generator rotor when the generator rotation axis is not eccentric, γ is the rotation angle of the generator rotor, i.e. $\cos\gamma = \frac{x_2}{e_2}$, $\sin\gamma = \frac{y_2}{e_2}$, $\varepsilon_2 = \frac{e_2}{\delta_0}$ is the rotor relative eccentricity, x_2, y_2 are the displacements of the generator rotor, and e_2 is the initial static eccentricity of the generator.

It can be seen from Eq.(2.5) that the unbalanced magnetic pull force has a strong nonlinearity with respect to the rotor displacement.

On the other hand, if the turbine is not symmetric or a periodic change occurs in the seal clearance of the machine's main shaft, the water pressure fluctuation within the seal will occur, which will result in an unbalanced force of water [4-7].

This force is:

$$p_{x_5} = k_w x,\ p_{y_5} = k_w y\,. \tag{2.6}$$

The water balance coefficient is denoted by k_w, where is the water imbalance coefficient [8, 9]. Linearizing the unbalanced magnetic traction force represented by Eq.(2.4) with the oil film force of the sliding bearing, we can add to the stiffness matrix K_r, and the unbalanced force of water in the turbine represented by Eq.(2.6) is also added to the stiffness matrix.

3. Simulation calculation of the critical rotational speed and the effect of stiffness

3.1. Calculation method of critical rotational speed

From Eq.(2.1), the free vibration equation of the system is [8]:

$$[M_r]\{\ddot{x}_r\} + [\omega_r G_r + C_r]\{\dot{x}_r\} + [K_r]\{x_r\} = 0\,. \tag{3.1}$$

Since the mass matrix, damping matrix and stiffness matrix in Eq.(3.1) are not all diagonal, the general method of computing the eigenvalues by solving the characteristic equation in the form of harmonic functions and finding the roots is not applicable.

We use the state variable method to solve this problem.

Introducing the state variables $V = [x_r,\ \dot{x}_r]^T$, Eq.(3.1) can be written as the following equation [8, 9]:

$$\dot{V} = \begin{Bmatrix} \dot{x}_r \\ \ddot{x}_r \end{Bmatrix} = \begin{Bmatrix} \dot{x}_r \\ -M_r^{-1}[(\omega_r G_r + C_r)\times \dot{x}_r + K_r \times x_r] \end{Bmatrix}. \tag{3.2}$$

In matrix form

$$\dot{V} = A \times V\,. \tag{3.3}$$

Here

$$\dot{V} = \begin{Bmatrix} \dot{x}_r \\ \ddot{x}_r \end{Bmatrix}, \qquad \mathrm{A} = \begin{Bmatrix} 0 & I \\ -M_r^{-1}\times K_r & -M_r^{-1}\times(\omega_r G_r + C_r) \end{Bmatrix} \tag{3.4}$$

The critical rotational speed of the system can be found by solving the singular value problem of matrix A in Eq.(3.3).

Setting the solution vector to

$$\boldsymbol{V} = \boldsymbol{A}e^{\lambda t} . \tag{3.5}$$

We have $dV / dt = \lambda V = \lambda \mathrm{A}e^{\lambda t}$ and Eq.(3.5) is expressed in the form $\mathrm{A} \cdot \mathrm{V}=\lambda \mathrm{V}$.

For example, in MATLAB, an eigenvalue solution of the form of Eq.(3.5) can be easily obtained for the singular value of the matrix A using the $[\,\mathrm{V}, \mathrm{D}\,]=\mathrm{eig}\,(\mathrm{A})$ command. The computed eigenvectors are contained in the main diagonal matrix D and the eigenvectors in the square matrix A.

Denoting the *i*-th eigenvalue of the system by $\lambda_i = u_i + i\omega$, the desired eigenvalue is a complex conjugate, and its imaginary part ω_i denotes the rotational angular frequency of the rotor at the specified rotational speed.

Using the imaginary part of the singular value, the critical rotational speed of the rotor can be found, and when the rotational speed of the rotor is equal to each other, ω_i is the rotational speed of the system i.

The real part u_i of the singular value is used to judge whether the system is stable or not, if all u_i is negative, the system is stable, and if the real part of at least one singular value is zero or positive, the system is unstable.

The procedure to calculate the critical rotational speed of the lateral vibration of the system is as follows. First, the initial speed of the rotor and the calculation time step are set, and the geometric and physical parameters of each element of the system are input.

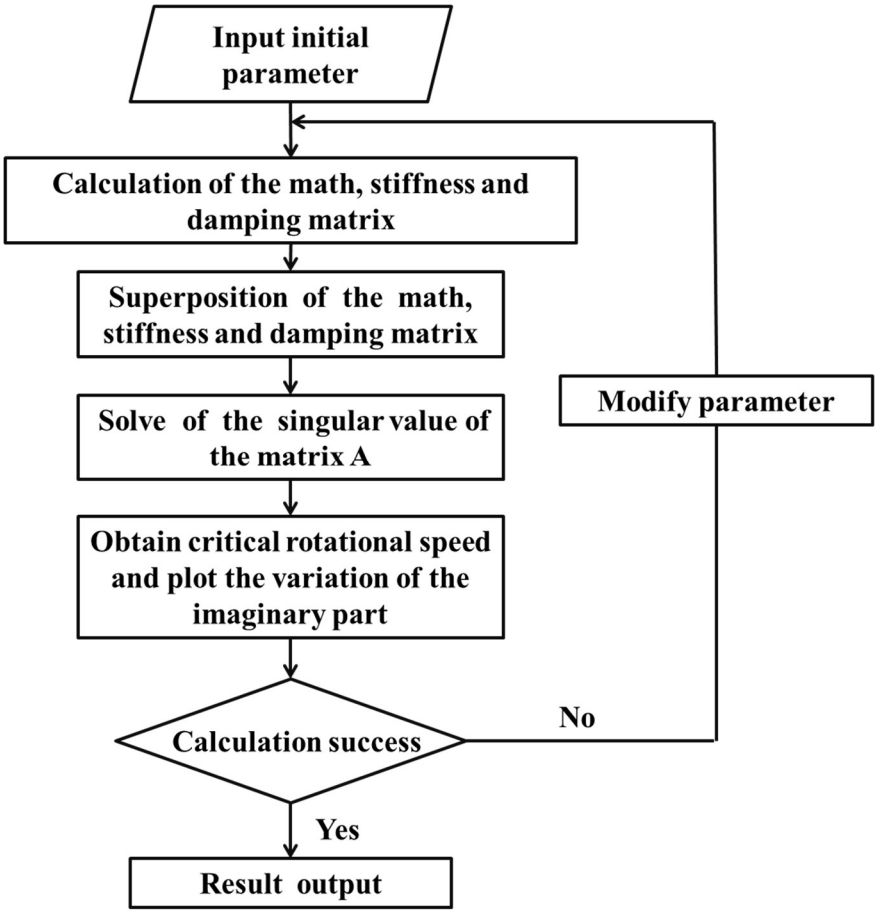

Fig.2. Flow chart for calculating the critical rotational speed.

Then, the element mass matrix and stiffness matrix are obtained and the element stiffness matrix of the sliding bearing is input.

Then, the mass and stiffness matrices of the whole system are obtained by superposition of the above element stiffness and mass matrices, and the singular values of A are obtained by using the MATLAB eigenvalue solver according to Eq.(3.3).

Plot the variation of the imaginary part of the singular value with the variation of the rotational speed and find the critical rotational speed of the lateral vibration of the system.

When the initial parameters do not meet the accuracy requirements in design and calculation, the initial parameters and calculation step time are reset to obtain the satisfied results.

The flowchart for calculating the critical rotational speed of the lateral vibration of the hydraulic turbine generator shaft system is shown in Fig.2.

3.2. Effect of sliding bearing stiffness on critical rotational speed

According to the method described above, the critical rotational speed of the hydraulic turbine generator shaft system is obtained and the effect of the sliding bearing stiffness on the critical rotational speed of the system is analyzed.

The system parameters are as follows:

Axis 1 in Fig.1 is considered as a hollow shaft with a constant cross-section, i.e., inner diameter is $I_d = 0.8\ m$, outer diameter is $O_d = 1.26\ m$, and length is $L = 1.6\ m$.

Shafts 2, 3 and 4 are one axis, with inner diameter is $I_d = 1.45\ m$ and outer diameter is $O_d = 1.9\ m$.

Where $L_1 = 4.5\ m$, $L_2 = 6.2\ m$ and $L_3 = 2.2\ m$.

The elastic modulus of the shaft is $E = 206\ GPa$, the density of the spindle is $7850\ kg/m^3$, the rotational speed of the spindle is $n = 75\ rpm$, the maximum rotational speed is $n = 145\ rpm$, the mass of the generator rotor is $m_1 = 1.2 \times 10^6\ kg$, the mass inertia is $4.5 \times 10^7\ kg \cdot m^2$, the aberration mass is $m_2 = 2.8 \times 10^5\ kg$ and the mass inertia is $2.4 \times 10^6\ kg \cdot m^2$ [1].

The critical rotational speed variation of the system is analyzed by varying the stiffness of the upper slide bearing, the lower slide bearing and the water wheel slide bearing.

For the simultaneous variation of the three sliding bearing stiffness, the coefficient of linearized unbalanced magnetic traction is fixed at $1.36 \times 10^8\ N/m$, and the sliding bearing is equivalent to an elastic system with stiffness and damping.

In Fig.3, the first and third Eigen modes of the system are shown.

Tab.1. Effect of three sliding bearing stiffnesses on the critical rotational speed (units: *r/min*).

Degree / stiffness *N/m*	1th	2th	3th
1×10^8	296.17	630.57	821.65
1.2×10^8	305.73	659.23	832.21
3.2×10^8	353.50	878.98	926.75
5.2×10^8	372.61	917.19	1 022.29
7.2×10^8	382.16	936.30	1 089.17
9.2×10^8	383.47	939.73	1 136.94
11.2×10^8	383.85	945.85	1 165.60

From Tab.1, it can be seen that when the bearing stiffness is increased from $1 \times 10^8 N/m$ to $11.2 \times 10^8 N/m$, the first, second and third critical rotational speeds are increased by *29%*, *49.9%* and *60%*, respectively, with the increase of bearing stiffness, the three critical rotational speeds of the system increase gradually and the increments are all relatively large.

Overall, the effect of the sliding bearing stiffness on the primary rotational speed of the system is relatively small and the effect on the tertiary critical rotational speed is relatively large.

It should be noted that the first and second critical rotational speeds nearly do not increase after the stiffness of $3.2\times10^8 N/m$.

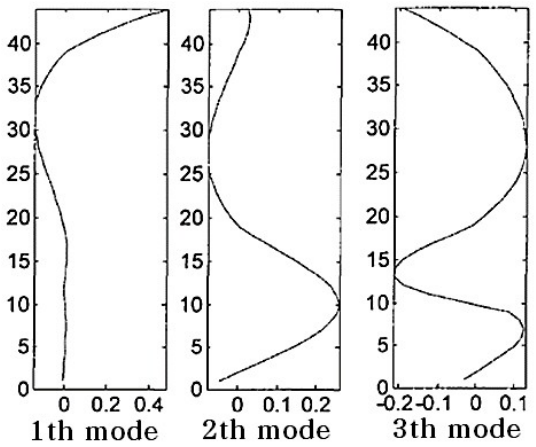

Fig.3. Natural vibration modes of a hydro-turbine generator.

- When only the stiffness of the upper slide bearing changes.

To analyze the effect of one slide bearing stiffness on the critical rotational speed of the system, the stiffness of the upper slide bearing is varied and the two slide bearing stiffness are fixed at $k = 7.2\times10^8 N/m$. Table 2 shows the effect of upper slide bearing stiffness on the critical rotational speed.

Tab.2. Effect of top slide bearing stiffness on critical rotational speed (in units: *r/min*)

Degree / stiffness *N/m*	1th	2th	3th
1.2×10^8	*382.16*	*936.30*	*1 089.17*
3.2×10^8	*382.85*	*936.84*	*1 089.53*
5.2×10^8	*383.21*	*937.28*	*1 090.17*
7.2×10^8	*383.95*	*938.14*	*1 090.83*
9.2×10^8	*384.54*	*938.91*	*1 091.37*
11.2×10^8	*385.29*	*939.47*	*1 092.12*

As can be seen from Tab. 2, increasing the upper slide bearing stiffness from $k = 1.2\times10^8 N/m$ to $k = 11.2\times10^8 N/m$ does not change the critical rotational speed of the system.

This indicates that the stiffness value of the upper slide bearing has little effect on the critical rotational speed of the system in the range considered above.

- When only the stiffness of the lower slide bearing changes.

Table 4 shows the influence of the lower slide bearing stiffness variation on the critical rotational speed when the upper and the aberration slide bearing stiffness is fixed at $k = 7.2 \times 10^8\ N/m$.

When the lower slide bearing stiffness is increased from $k = 1.2 \times 10^8\ N/m$ to $k = 11.2 \times 10^8\ N/m$, the critical rotational speeds increase considerably, with the second critical rotational speed increasing by about *36%* and the third critical rotational speed increasing by about *20%*.

When the lower slide bearing stiffness is greater than $k = 7.2 \times 10^8\ N/m$, the first and second critical rotational speeds remain constant with the increase of bearing stiffness.

Tab.3. Influence of lower slide bearing stiffness on critical rotational speed (unit: *r/min*).

Degree / stiffness *N/m*	1th	2th	3th
1.2×10^8	*343.94*	*687.89*	*955.41*
3.2×10^8	*371.34*	*878.98*	*984.07*
5.2×10^8	*372.61*	*926.75*	*1 041.40*
7.2×10^8	*376.51*	*936.30*	*1 089.17*
9.2×10^8	*380.31*	*938.48*	*1 127.38*
11.2×10^8	*382.16*	*940.21*	*1 146.49*

The first and second critical rotational speeds are almost constant for stiffness values above $5.2 \times 10^8\ N/m$.

- When only the turbine sliding bearing stiffness changes.

When the upper and lower slide bearings stiffness are fixed at $k = 7.2 \times 10^8\ N/m$, Tab.4 shows the effect of the aberration slide bearing stiffness on the critical rotational speed: the first critical rotational speed increases by about *14.3%*, the second by about *12.6%*, and the third critical rotational speed increases by about *10.4%*.

Tab.4. Critical rotational speed (in units: *r/min*) as a function of the rotor sliding bearing stiffness.

Degree / stiffness *N/m*	1th	2th	3th
1.2×108	*334.39*	*831.21*	*1 003.18*
3.2×108	*363.05*	*907.64*	*1 041.4*
5.2×108	*372.61*	*926.75*	*1 070.06*
7.2×108	*382.16*	*936.30*	*1 089.17*
9.2×108	*384.38*	*938.71*	*1 098.72*
11.2×108	*386.31*	*941.61*	*1 108.28*

The critical rotational speeds of the first, second and third orders are constant after the stiffness is $3.2 \times 10^8\ N/m$.

A comprehensive analysis of the effect of a single slide bearing on the critical rotational speed of the system shows that, in general, the critical rotational speed of the system increases with the increase of the sliding bearing stiffness; however, there exists a limit at which the first and second critical rotational speeds become almost constant when the increase of the sliding bearing stiffness reaches a certain extent.

Therefore, an overall increase in the sliding bearing stiffness does not always lead to an increase in the critical rotational speed of the system, and should be chosen reasonably according to the system characteristics, which depend on the system characteristics and can be determined based on the above analysis.

4. Field tests and results analysis

The results of the field test analysis are illustrated to demonstrate the validity of the results for the simulation study of the mathematical model.

The hydro-turbine generator (rated power *10 MW*, speed *410 r/min*, maximum head *390 m*) of a hydro-electric power plant in our country was in a state of water operation where the vibration level of each sliding bearing of the generator exceeded the allowable limit (*100* μ*m*) and caused severe vibration and was difficult to operate.

Based on the standard design dimensions of the hydro-turbine generator, the first critical rotational speed is *16.5 Hz* and the second critical rotational speed is *39.6 Hz*, calculated by the aforementioned method. The vibration level of each slide bearing measured during operation is shown in Tab.5.

Tab.5. Vibration level of vibration measurement points (in units: μ*m*).

Measurement position	Upper slide bearing	Lower slide bearing	Turbine slide bearing
Level	*150*	*210*	*138*

The real waveform and spectral diagram at the measurement points are shown in Fig.4 and the axial diagram in Fig.5.

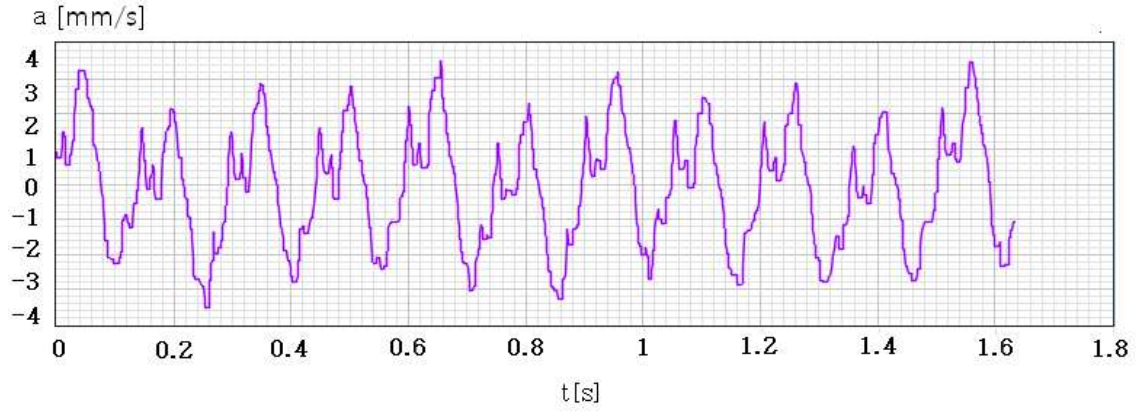

a) Vibration speed signal waveform of upper slide bearing.

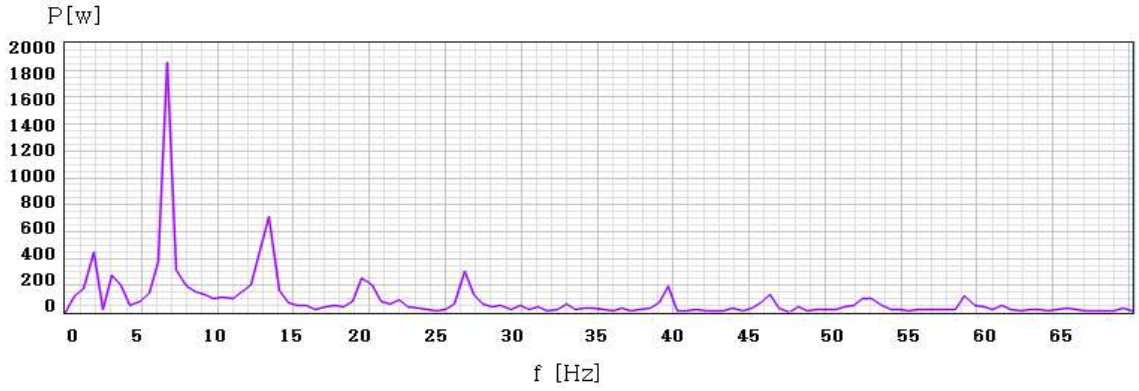

b) Power spectrum of upper slide bearing vibration speed signal (Fig.4.a).

Fig.4. Vibration velocity signals and spectrogram at the measurement points.

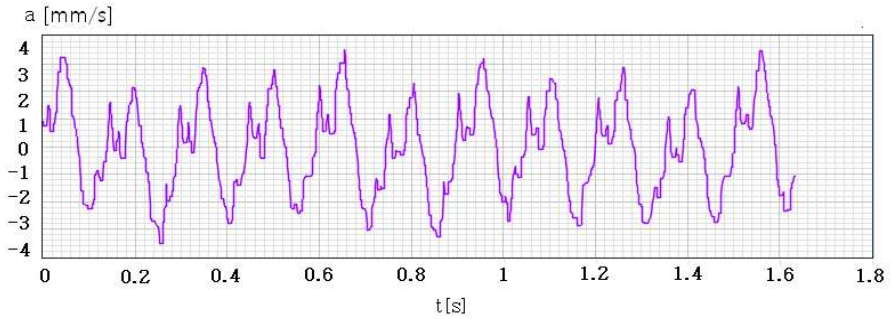

c) Vibration speed signal waveform of lower slide bearing.

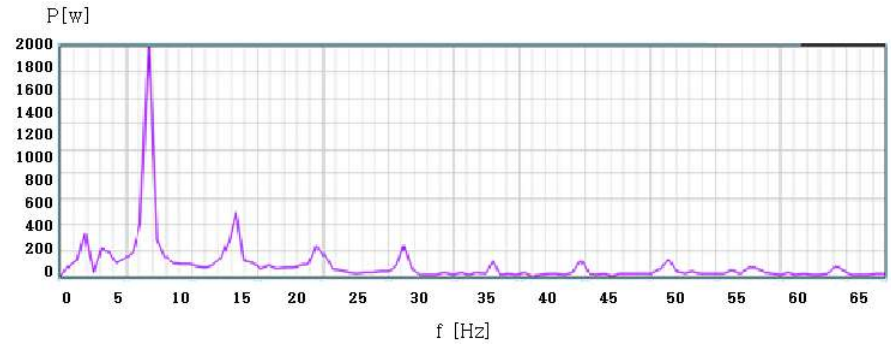

d) Power spectrum of lower slide bearing(Fig.4.c)

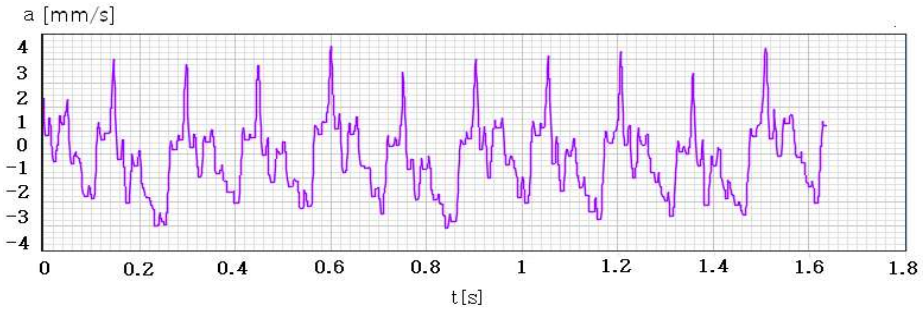

e) Vibration speed signal waveform of the water wheel slide bearing.

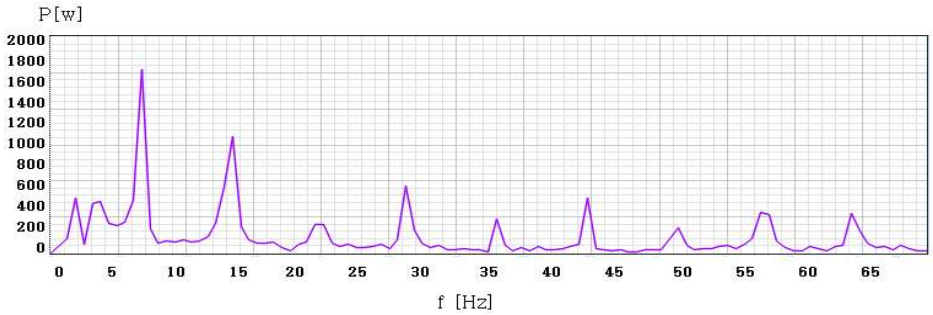

f) Spectrum of the water wheel sliding bearing.

Fig.4 cont. Vibration velocity signals and spectrogram at the measurement points.

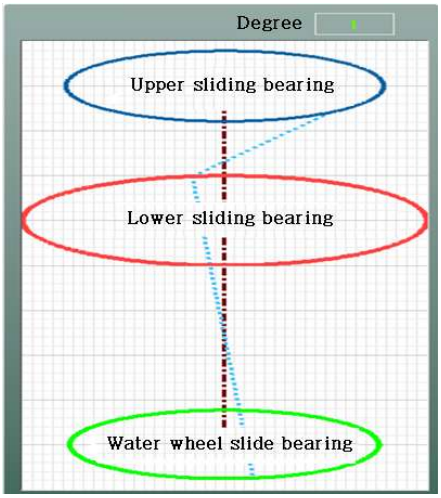

Fig.5. Axial diagram of the generator-turbine shaft system.

From the vibration levels, spectral diagrams and axial diagrams of the measuring positions, it can be seen that the rotation axis has strong bending vibration and the mode of bending vibration coincides with the first natural mode of the axial system, and the first resonance occurs.

Inspection of the assembly state of the turbo-generator showed that the assembly dimensions and radial clearances of the upper, lower and aberration sliding bearings did not reach the design level, which reduced the stiffness, thus reducing the system's first critical rotational speed.

Based on the results calculated in the previous section, the bearings that have a decisive influence on the critical speed of the system are the lower and the water wheel bearings, so based on the design-level dimensions of the turbine generator assembly, the assembly dimensions of the lower and water wheel sliding bearings and the oil film clearance are adjusted to the design value, and the turbine generator is reassembled to drive the turbine generator, the vibration is reduced to the steady level ($50\ \mu m$), the shaft diagram of the generator-turbine shaft system shown in Fig.5 is not shown, and the primary resonance is eliminated.

This is because in this case the first and second critical rotational frequencies are far enough away from the turbine rotational frequency of $6.83\ Hz$, which shows the validity of the aforementioned critical rotational frequency calculation method.

5. Conclusions

A dynamic model representing a system of nonlinear differential equations considering various coupling actions for a hydro-turbine spindle system was established, the effect of the sliding bearing stiffness on the critical rotational speed of the system was studied, and field tests demonstrated the validity of the theoretical findings.

When the stiffness of the three sliding bearings supporting the system is increased simultaneously, the critical rotational speed of the system is generally increased, but the degree depends on the order of the critical rotational speed.

Regarding the effect of the stiffness of individual bearings on the critical rotational speed, the upper slide bearing has little effect on the critical rotational speed of the system, but the increase of the stiffness of the lower bearing and turbine bearing increases the critical rotational speed relatively significantly.

However, when the sliding bearing stiffness is large to some extent, there is a limit at which the first and second critical rotational speeds no longer increase, and it is difficult to prevent resonance by increasing the critical rotational speed of the system by increasing the bearing stiffness.

Therefore, in order to achieve vibration stability by increasing the critical rotational speed of the system sufficiently, it is necessary to increase the stiffness of the support bearings and also improve other factors such as the mass of the system, the sectional properties of the shaft and damping.

This has been verified through a field application example.

Nomenclature

C_r – damping matrix,
E – Young's modulus of the shaft material,
G_r – gyroscopic matrix,
I_i – axial moment of inertia of the cross section of shaft i,
I_j – field current of the generator rotor,
J_{di}, J_{pi} – axial and polar moments of inertia of mass i
K_j – air gap fundamental magnetic intensity coefficient,
K_r – stiffness matrix
l_i – length of shaft link E_i
L_r – length of the rotor,
M_r – mass matrix of the system,
R_r – radius of the generator rotor,
x_2, y_2 – displacements of the generator rotor
δ_0 – average air-gap of the generator rotor
Λ_n – expansion coefficient
μ_0 – magnetic induction coefficient in the air,
ω_r – angular velocity of the shaft system,

References

[1] Sheng X., Li B., Wu Z. and Li H. (2014): *Calculation of ball bearing speed-varying stiffness*.– Mechanism and Machine Theory, vol.81, pp.166-180.

[2] Li J. and Chen Q. (2014): *Nonlinear dynamical analysis of hydraulic turbine governing systems with nonelastic water hammer effect*.– Journal of Applied Mathematics, ArticleID 412578, p.11, https://doi.org/10.1155/2014/412578.

[3] Gustavsson R. and Aidanpää J.-O. (2006): *The influence of nonlinear magnetic pull on hydropower generator rotors*.– Journal of Sound and Vibration, vol.297, No.3, pp.551-562.

[4] Wu W., Pang J., Liu X., Zhao W., Lu Z., Yan D., Zhou L. and Wang Z. (2023): *Effect of unbalanced magnetic pull of generator rotor on the dynamic characteristics of a pump-turbine rotor system*.– Water, vol.15, No.6, p.1120, https://doi.org/10.3390/w15061120.

[5] Toliyat H.A., Nandi S., Choi S. and Meshgin-Kelk H. (2013): *Electric Machines Modeling, Condition Monitoring, and Fault Diagnosis*.– CRC Press, Taylor & Francis, p.227.

[6] Li Q., Zhang S., Ma L., Xu W. and Zheng S. (2017): *Stiffness and damping coefficients for journal bearing using the 3D transient flow calculation*.– Journal of Mechanical Science and Technology, vol.31, No.5, pp.2083-2091, https://doi.org/10.1007/s12206-017-0405-9.

[7] Zhang X., Yin Z. and Gao G. (2015): *Determination of stiffness coefficients of hydrodynamic water-lubricated plain journal bearing*.– Tribology International, vol.85, pp.37-47, https://doi.org/10.1016/j.triboint.2014.12.019.

[8] Alves V.C.A., Alves D.S. and Machado T.H. (2022): *Linear and nonlinear performance analysis of hydrodynamic journal bearings with different geometries*.– Appl. Sci., vol.12, No.7, p.3215, https://doi.org/10.3390/app12073215.

[9] Ling F.F. (2005): *Dynamics of Rotating Systems*.– Mechanical Engineering Series, pp.298-315.

[10] Keyun Z., Gao Ch., Li Z., Yan D. and Fu X. (2018): *Dynamic analyses of the hydro-turbine generator shafting system considering the hydraulic instability*.– Energies, vol.11, No.10, p.2862, https://doi.org/10.3390/en11102862.

[11] Rebelein C., Vlacil J. and Zaeh M.F. (2017): *Modeling of dynamic behavior of machine tools; influence of damping, friction, control and motion*.– Prod. Eng. Res. and Develop., vol.11, pp.61-71, DOI:10.1007/s11740-016-0704-5.

[12] Wang W., Shang Y. and Yao S. (2022): *A predictive analysis method of shafting vibration for the hydraulic-turbine generator unit*.– Water, vol.14, No.17, p.2714, https://doi.org/10.3390/w14172714.

[13] Bai B., Zhang L.X. and Zhao L. (2012): *Influences of the guide bearing stiffness on the critical speed of rotation in the main shaft system*.– IOP Conference Series: Earth and Environmental Science, vol.15, No.7, p.072028, IOP Publishing, https://doi.org/10.1018/1755-1315/15/7/072028.

[14] Pal T.K., Ray A., Chowdhury S.N. and Ghosh D. (2023): *Extreme rotational events in a forced-damped nonlinear pendulum*.– Chaos: An Interdisciplinary Journal of Nonlinear Science, vol.33, No.6, p.10, https://doi.org/10.48550/arXiv.2304.00039.

Received: October 21, 2024
Revised: July 12, 2025